Geochemical Characteristics of the Trace and Rare Earth Elements in Reef Carbonates from the Xisha Islands (South China Sea): Implications for Sediment Provenance and Paleoenvironment

BI Dongjie[1], ZHAI Shikui[1], [*], ZHANG Daojun[2], XIU Chun[3], LIU Xinyu[2], LIU Xiaofeng[1], JIANG Longjie[1], and ZHANG Aibin[1]

1) *Key Laboratory of Submarine Geosciences and Prospecting Techniques*, *Ministry of Education*, *College of Marine Geosciences*, *Ocean University of China*, *Qingdao* 266100, *China*
2) *Zhanjiang Branch Institute of China National Offshore Oil Corporation (CNOOC) Limited*, *Zhanjiang* 524057, *China*
3) *North China Sea Environmental Monitoring Center*, *Ministry of Natural Resources*, *Qingdao* 266033, *China*

© Ocean University of China, Science Press and Springer-Verlag GmbH Germany 2019

Abstract   Based on the concentrations of the trace elements, rare earth elements (REE), and Sr isotopic compositions in reef carbonates from the well 'Xike-1' reef core of the Xisha Islands, the constraints on sediment provenance and paleoenvironment were defined. Variations of the terrigenous input into the paleoseawater were traced in detail and the paleoenvironment and sediment provenance were further investigated. The results show that the HREE/LREE values in the reef carbonates are negatively associated with their Th and Al concentrations; however, their Al and Th concentrations show positive correlation. The lowest $^{87}Sr/^{86}Sr$ values in the reef carbonates generally coincide with the lowest values of Al, Th concentrations and the highest values of HREE/LREE. These data indicate that the HREE/LREE, Al concentrations, and Th concentrations of the reef carbonates are useful indexes for evaluating the influence of the terrigenous inputs on the seawater composition in the study area. From top to bottom, the changing process of the HREE/LREE values and Al, Th concentrations can be divided into 6 intervals; they are H1 (0–89.30 m, about 0–0.11 Myr), L1 (89.30–198.30 m, about 0.11–2.2 Myr), H2 (198.30–374.95 m, about 2.2–5.3 Myr), D (374.95–758.40 m, about 5.3–13.6 Myr), L2 (758.40–976.86 m, about 13.6–15.5 Myr), and H3 (976.86–1200.00 m, about 15.5–21.5 Myr). Moreover, the changing trend of the HREE/LREE values coincides with that of the seawater $\delta^{13}C$ values recorded by benthonic foraminiferal skeletons from the drill core of ODP site 1148 in the South China Sea (SCS), but not with that of the seawater $\delta^{18}O$ values. The high uplifting rates of the Qinghai-Tibet Plateau coincide with the high Th and Al concentrations and the low HREE/LREE values in the reef carbonates. These data indicate that the main factors controlling the changes of terrigenous flux in the SCS are the tectonic activities associated with Qinghai-Tibet Plateau uplifting and the variations of uplifting rates rather than paleoclimatic changes.

Key words   trace and rare earth elements; paleoenvironmental and sediment provenance; reef carbonates; the South China Sea (SCS); the uplift of Qinghai-Tibet Plateau

1 Introduction

The trace elements, rare earth elements (REE) and isotopic compositions of chemical precipitates (*e.g.*, carbonate, phosphate, and chert) can record the geochemical characteristics of paleoseawater. The geochemical characteristics of seawater are dictated by a number of factors such as the changes of terrigenous influx, the physicochemical property of elements, paleoclimatic changes, and biological activities. Thus, the temporal and spatial variations of elemental and isotopic compositions of paleoseawater can

provide important information for reconstructing the paleoclimatic and paleoenvironmental changes of the earth surface system. Elements and isotopes with known behaviors in modern marine sediments have been extensively utilized to reconstruct the geochemical characteristics of paleoseawater or to trace the changes of paleoclimate and paleoenvironment in the geological history. Previous studies have shown that Mg/Ca, Sr/Ca, and U/Ca values of coral skeletons can be used to estimate the variability of seawater surface temperatures (Wei *et al.*, 2000; Armid *et al.*, 2011). The V/Ca values of foraminiferal skeletons can be used to decipher the areal extent of anoxic and suboxic sediments (Hastings *et al.*, 1996; Morford and Emerson, 1999), and the P/Ca values of coral skeletons can be used to estimate the phosphate concen-

tration of seawater and to trace the upwelling (Chen and Yu, 2011; Anagnostou *et al.*, 2011).

Marine carbonates can absorb trace elements in their crystal lattices, whose concentrations dependent on the geochemical compositions of seawater and the partition coefficients between carbonate and seawater (Zhao and Zheng, 2014). The insoluble elements, such as Be, Al, Sc, Co, Ga, Cs, REE, Hf, and Th, mainly relate to the terrigenous detritus and can not be incorporated into carbonate lattices (Zhao and Zheng, 2014), which can provide a proxy for contributions from terrigenous materials (Webb and Kamber, 2000; Kamber *et al.*, 2004; Frimmel, 2009; Zhao *et al.*, 2009). Thus, the paleoenvironment and sediment provenance can be further investigated. However, because of the limit of samples, most of the researches employing this method focused on the ancient carbonate platforms and short-term variations in previous studies (*e.g.*, Xi *et al.*, 2005; Zhao and Zheng, 2014).

Carbonate platforms, which represent one of the most important types of reservoirs, comprise high volume of biogenic sediments and are widespread in tropical and subtropical areas; they are especially widespread in the clear shallow waters of Southeast Asia, such as the South China Sea (SCS) (Umbgrove, 1947; Bachtel *et al.*, 2004). The coral reefs in Xisha area started to form at about 23 Myr (Xia, 1996; Zhang *et al.*, 2003), which are still developing. Thus, the continuous growing coral reefs provide the basic samples for reconstructing the long-term influx variations of terrigenous materials in the SCS. In this article, based on the concentrations of the trace elements and REEs, and isotopic compositions in reef carbonates from the well 'Xike-1' reef core of the Xisha Islands, the constraints on sediment provenance and paleoenvironment were defined. Variations of the terrigenous input into the paleoseawater were traced in detail and the paleoenvironment and sediment provenance were further investigated.

2 Geologic Setting

The South China Sea is the largest marginal sea in the western Pacific Ocean, which exists in a semi-enclosed environment. It is connected to the East China Sea by the Taiwan Strait and connects to the Pacific Ocean through the Luzon Strait, which is located in the southern region of the South China continent (Wang *et al.*, 2018; Xie *et al.*, 2018). The uplift of Qinghai-Tibet Plateau and the formation of SCS basin were produced by tectonic movements in almost the same geological period (Wang *et al.*, 2015). The special geographical location and the rapid depositional feature (Sarnthein *et al.*, 1994) amplify the responses to global paleoclimatic and paleoenvironmental changes in the SCS (Zhao and Wang, 1999). Due to its unique position, the SCS has been shown to be one of the most significant regions for carbonate platform development since the Miocene (Shao *et al.*, 2017).

The Xisha Islands (17°07′–15°43′N, 111°11′–112°54′E) are located on an elevated submarine plateau, which rises from the lower slope at the southeast of Hainan Island.

Scientific and commercial drilling programs conducted in the 1970s and 1980s provided extensive data for describing the biostratigraphy, lithology, sedimentology, paleomagnetism, and seismology of the islands, as well as the information about the morphology of their biota (Wang *et al.*, 1979; Zhang *et al.*, 1994; Liu *et al.*, 1997; Zhao *et al.*, 2001; Shi *et al.*, 2002). However, these early boreholes were limited in their utility due to incomplete core recovery and a lack of basement drilling.

Well 'Xike-1' is located on Shi Island of the Xuande Atoll, Xisha Islands (16°50′45″N, 112°20′50″E; Fig.1). The designated drilling depth is 1300 m, with complete core recovery and basement drilling. The total length of the drilling core is 1268.02 m and the average rate of core recovery is approximately 80%. Thus far, this site represents the deepest scientific drilling site, with the highest rate of core recovery, in the Xisha area, which provides the basic samples for analyzing the geochemical characteristics of the reef carbonates, continuously. In addition, the paleoenvironment and sediment provenance can be further investigated.

3 Samples and Analytical Methods

The samples in this study are from the well 'Xike-1' reef core. The logging and core data of the well 'Xike-1' indicate that the core sediments below 1200 m are mainly breccia with mudstone and argillaceous fine sandstone. Mineral compositions of the reef core also indicate that the concentrations of non-carbonate minerals (*e.g.*, quartz, feldspar, mica, kaolinite, and montmorillonite) are relatively high during this interval (Xiu, 2016). This indicates that the early environment of reef-forming was fringing reef or patch reef, which was significantly influenced by terrigenous detritus. However, the core sediments mainly consist of pure carbonate in the section above 1200 m, whose mineral compositions are mainly carbonate minerals (*e.g.*, calcite, aragonite, and dolomite) (Zhai *et al.*, 2015; Xiu, 2016). In detail, high-magnesian calcites appear in the segment of 0–36.00 m. Aragonites mainly appear in the segments of 0–36.00 m and 207.30–241.30 m (Figs.2B and 2C), but the aragonites in the segment of 207.30–241.30 m are fibroid aragonites, which were produced by cementation instead of protosomatic process (Fig.2B). Dolomites appear in the segment below 181.25 m (Figs.2D, 2E and 3). Thus, the drilled reef sediments generally suffered from two stages of diagenesis: transformation from aragonite to calcite (calcitization) and further into dolomite (dolomitization). Moreover, the island where well 'Xike-1' is located has been isolated from the main continent since the formation of the Xisha Block during the early Cenozoic (Shao *et al.*, 2017). Therefore, the geochemical characteristics of trace elements and REEs in the reef carbonates from the segment above 1200 m can be used to trace the paleoenvironment and the paleoseawater chemical properties.

Based on the principle of equidistant sampling and the principle of increasing sampling density in the vicinity of lithostratigraphic boundaries, 266 samples were selected

for X-ray fluorescence (XRF) analysis to obtain the major elemental composition data; and 466 samples were selected for inductively coupled plasma mass spectrometry (ICP-MS) analysis to obtain the trace element and REE composition data (the analysis methods and procedures were described in detail by Xiu *et al.* (2015) and Xiu (2016)).
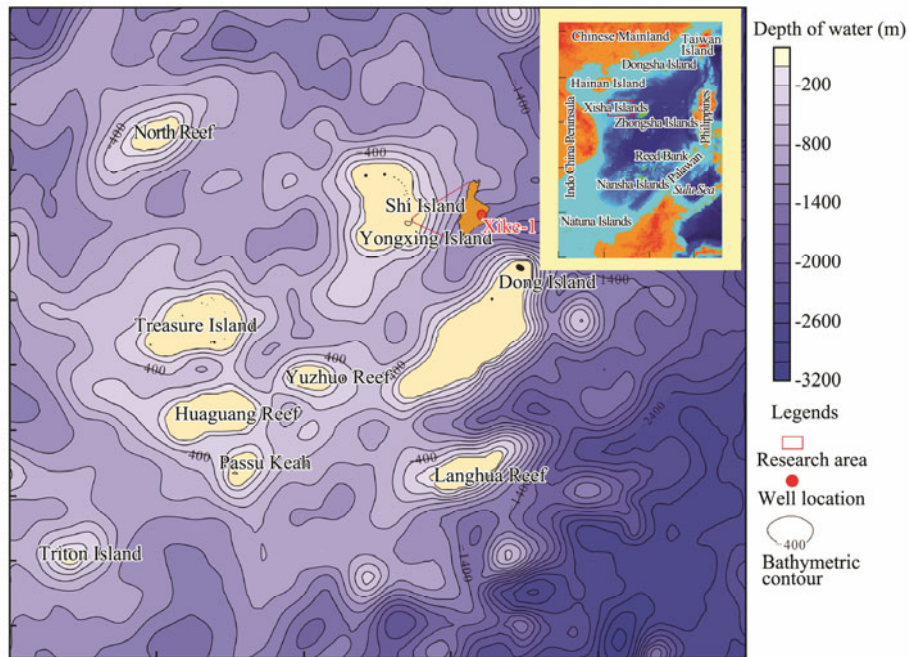

Fig.1 The location of the well 'Xike-1' and its lithologic section. It was modified from the data provided by Zhanjiang Branch of CNOOC Ltd.
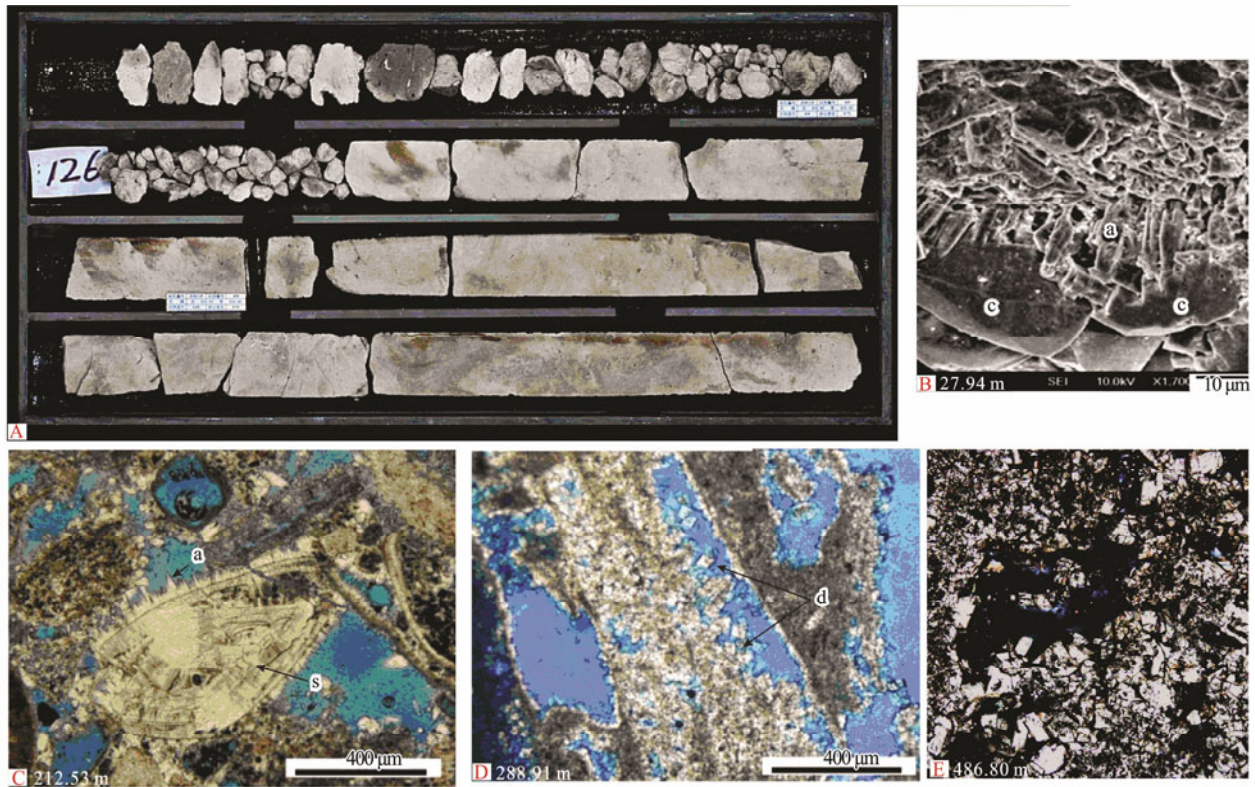

Fig.2 Geological features of carbonates in the well 'Xike-1' reef core. (A), The well 'Xike-1' reef core. (B), Microphotographs under scanning electron microscope for samples in the well 'Xike-1' reef core. (C), (D), and (E), Microphotographs in plane-polarized light for samples in the well 'Xike-1' reef core. (B), The cementation of calcite and aragonite. (C), The fibroid aragonites. (D), The cementation of dolomite. (E), Microphotograph of the sample from the dolomite layer. (B), (C), and (D) are provided by Zhanjiang Branch of CNOOC Ltd. a, aragonite; c, calcite; d, dolomite; s, skeleton.

4 Results

The stratigraphic classification of the well 'Xike-1' reef core is provided by the Zhanjiang Branch of CNOOC Ltd. (Fig.1), which was divided based on the seismic data. At those stratigraphic and chronologic boundaries, the diagenetic environment (Wang *et al.*, 2015; Zhao *et al.*, 2015), concentrations of elements (major, trace, and rare earth elements) (Xiu *et al.*, 2015), mineral compositions (Zhai *et al.*, 2015), and isotopic compositions (Qiao *et al.*, 2015; Zhu *et al.*, 2015; Bi *et al.*, 2017) of the reef carbonates manifest as sudden changes, and the fossil assemblages in the reef core also show as significant changes (Ma *et al.*, 2015). Moreover, those boundaries coincide with the exposure surfaces that identified in the reef core (You *et al.*, 2015). Thus, those stratigraphic and chronologic boundaries are affirmed by the mineralogical, geochemical, and paleontological data of the well 'Xike-1' reef core, and the depth and chronologic data are extracted for contrastive researches.

The results show that the concentrations of the trace elements and REEs in reef carbonates from the intervals above 1200 m are different from those from the interval below 1200 m (Tables 1 and 2). The HREE/LREE values in the reef carbonates from the interval above 1200 m range from 0.01 to 0.57, with an average value of 0.24. The concentrations of Th, Al, Sr, Fe, and Mn in the interval above 1200 m range from 0 to 1.50×10^{-6}, 0.01% to 0.47%, 44.00×10^{-6} to 8803.52×10^{-6}, 0.01% to 0.71%, and 7.75×10^{-6} to 309.86×10^{-6}, respectively. The average concentrations of Th, Al, Sr, Fe, and Mn are 0.19×10^{-6}, 0.05%, 937.82×10^{-6}, 0.04%, and 35.87×10^{-6}, respectively. The PAAS-normalized HREE/LREE values of the reef carbonates range from 1.17 to 3.42, with an average value of 2.38. The average PAAS-normalized HREE/LREE values of the reef carbonates are 1.17, 3.42, 2.95, 2.29, 2.53, and 1.90 in the intervals of H1, L1, H2, D, L2, and H3, respectively.

5 Discussion

5.1 Evaluation of Diagenetic Alteration

The elemental and isotopic compositions of the marine carbonates might be modified by diagenetic alteration. Thus, the effects of diagenesis on the elemental and iso-

Table 1 Variation ranges and average values of the concentrations of trace elements and REEs
in the reef carbonates from the well 'Xike-1' reef core

Series and depth		HREE/LREE	Th×10⁻⁶	Al (%)	Sr×10⁻⁶	Fe (%)	Mn×10⁻⁶
Pleistocene–Holocene (0–214.89 m)	Max	0.57	1.50	0.47	7457.33	0.40	139.44
	Min	0.01	0.01	0.01	414.87	0.01	15.49
	Ave	0.21	0.21	0.06	2008.60	0.04	45.03
Pliocene (214.89–374.95 m)	Max	0.41	0.39	0.12	1635.47	0.13	69.72
	Min	0.16	0.05	0.03	200.25	0.01	23.24
	Ave	0.26	0.17	0.06	571.25	0.04	39.33
Upper Miocene (374.95–576.50 m)	Max	0.35	1.49	0.10	694.12	0.16	85.21
	Min	0.14	0.05	0.02	166.49	0.01	15.49
	Ave	0.22	0.20	0.02	226.40	0.01	15.49
Middle Miocence (576.50–1032.16 m)	Max	0.46	0.90	0.22	702.17	0.16	69.72
	Min	0.20	0.00	0.01	44.00	0.01	7.75
	Ave	0.28	0.14	0.04	330.78	0.02	27.40
Lower Miocene (1) (1032.46–1200.00 m)	Max	0.32	0.66	0.29	8803.52	0.71	309.86
	Min	0.06	0.06	0.01	142.62	0.01	15.49
	Ave	0.22	0.26	0.06	430.25	0.07	50.00
Lower Miocene (2) (1200.00–1257.52 m)	Max	0.18	18.38	10.86	666.55	4.43	883.10
	Min	0.05	0.32	0.05	119.75	0.03	30.99
	Ave	0.10	4.13	1.82	323.04	0.85	241.38
0–1200.00 m	Max	0.57	1.50	0.47	8803.52	0.71	309.86
	Min	0.01	0.00	0.01	44.00	0.01	7.75
	Ave	0.24	0.19	0.05	937.82	0.04	35.87

Table 2 Average PAAS-normalized REE concentrations in carbonate samples from the 6 intervals
(L1, L2, D, H1, H2, and H3) in well 'Xike-1' reef core

Intervals	PAAS-normalized REE concentrations														
	La	Ce	Pr	Nd	Sm	Eu	Gd	Tb	Dy	Ho	Er	Tm	Yb	Lu	HREE/LREE
H1	0.04	0.36	0.04	0.04	0.06	0.01	0.10	0.09	0.08	0.08	0.08	0.10	0.07	0.07	1.17
L1	0.01	0.01	0.02	0.02	0.03	0.00	0.03	0.04	0.04	0.04	0.04	0.05	0.03	0.03	3.42
H2	0.02	0.01	0.02	0.02	0.04	0.00	0.04	0.05	0.05	0.05	0.05	0.05	0.04	0.04	2.95
D	0.02	0.01	0.02	0.02	0.03	0.02	0.04	0.04	0.04	0.04	0.04	0.03	0.02	0.02	2.29
L2	0.02	0.01	0.02	0.02	0.04	0.03	0.05	0.05	0.05	0.05	0.05	0.05	0.03	0.03	2.53
H3	0.04	0.02	0.03	0.03	0.06	0.06	0.06	0.06	0.07	0.05	0.07	0.06	0.05	0.04	1.90

topic compositions should be evaluated. Previous studies have shown that the strong diagenetic alteration would greatly change the primary geochemical features of the marine carbonate (Veizer and Compston, 1974; Hess *et al*., 1986). Numerous studies have indicated that the elemental concentrations of Sr are important indicators for evaluating the degree of diagenetic alteration, including the effects of meteoric diagenesis and dolomitization (Kaufman and Knoll, 1995). Generally, Sr tends to be expelled out of marine carbonates during diagenesis (Li *et al*., 2011; Edwards *et al*., 2015). The Sr concentrations in the reef carbonates range from 44.00×10^{-6} to 8803.52×10^{-6}, with an average value of 936.27×10^{-6} (Table 1). The samples with Sr concentrations lower than 200×10^{-6} are mainly composed of dolomites (whose dolomite concentrations >70%) (Fig.3), due to their lower Sr distribution coefficient (Huang *et al*., 2008). The Sr concentrations in most samples are much higher than the minimum Sr concentration (200×10^{-6}) for strontium-isotope stratigraphy research suggested by Derry *et al*. (1989). Thus, the reef carbonates from the well 'Xike-1' reef core could record the geochemical compositions of seawater. Another principal geochemical signal, which is sensitive to diagenetic alteration, is the oxygen isotopic composition. The oxygen isotopic compositions of the marine carbonates tend to decrease during isotopic exchange with meteoric or hydrothermal fluids (Kaufman *et al*., 1993). The $\delta^{18}O$ values ranging from 0 to $-5‰$ are observed in the least altered limestones. Values less than $-5‰$ would represent a mild degree of alteration, while those below $-10‰$ are considered to be unacceptably altered (Kaufman *et al*., 1993). Shao *et al*. (2017) reported that the $\delta^{18}O$ values of reef carbonates from the well 'Xike-1' reef core range from $-9.18‰$ to $4.77‰$, which do not belong to unacceptably altered carbonate.
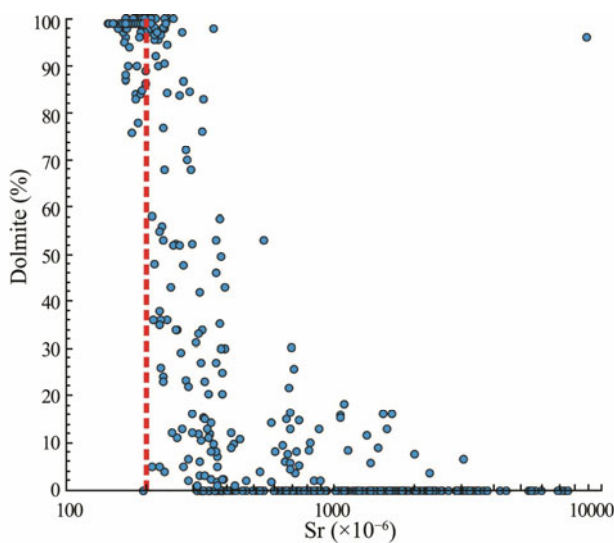

Fig.3 Cross plots of dolomite *vs*. Sr for reef carbonates from the well 'Xike-1' reef core. The red line represents the Sr concentration of 200×10^{-6}.

Diagenetic alteration can also increase the Mn and Fe concentrations of the marine carbonates, when they are influenced by the atmospheric water cycle (Brand and Veizer, 1980, 1981; Bruckschen *et al*., 1995). Thus, the Fe and Mn concentrations and Mn/Sr values in the marine carbonates are useful proxies to estimate the degree of diagenetic alteration (Li *et al*., 2011; Edwards *et al*., 2015). The Fe concentrations of reef carbonates from the well 'Xike-1' reef core are low. The Mn concentrations in most samples are much lower than the maximum Mn concentration (250×10^{-6}) for seawater geochemical research suggested by Korte *et al*. (2013). Only one sample exhibits relatively high Mn concentration ($> 250 \times 10^{-6}$), but exhibits relatively low Fe concentration (Fig.4), so the effects of diagenesis can be excluded. Moreover, according to Kaufman *et al*. (1992, 1993), the Mn/Sr values above 2–3 are observed in the unacceptably altered carbonate, which can not be used to reconstruct the paleoenvironment. The Mn/Sr values in the reef carbonates from 'Xike-1' reef core range from 0.0041 to 1.4515, which indicates that reef carbonates from the well 'Xike-1' reef core can record the primary geochemical compositions of seawater.
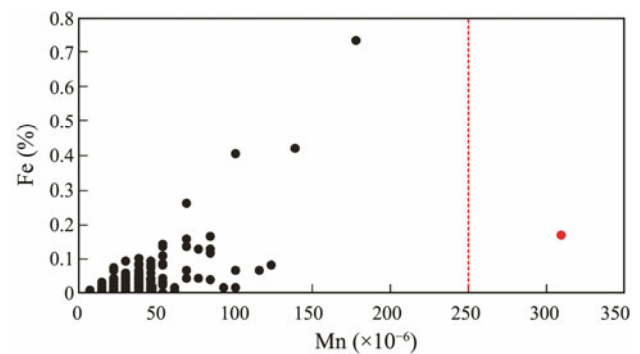

Fig.4 Cross plots of Fe *vs*. Mn concentrations for reef carbonates from the well 'Xike-1' reef core. The red line represents the Mn concentration of 250×10^{-6}.

The drilled reef sediments generally suffer from two stages of diagenesis: transformation from aragonite to calcite (calcitization) and further into dolomite (dolomitization). Previous studies have shown that the correlation between the mineral compositions and the concentrations of elements (trace elements and REE) or other geochemical indicators (Xiu *et al*., 2015; Zhai *et al*., 2015; Shao *et al*., 2017) was poor. This indicates that the reef carbonates were not significantly influenced by diagenetic alteration, and they recorded their primary geochemical characteristics. These data indicate that all the samples from the well 'Xike-1' reef core are not significantly altered by burial or meteoric diagenesis and they keep their original geochemical characteristics.

5.2 Changes of the Terrestrial Detritus Input into the SCS

The insoluble elements, such as Be, Al, Sc, Co, Ga, Cs, REE, Hf, and Th, mainly relate to the terrigenous detritus and can not be incorporated into carbonate lattices (Zhao and Zheng, 2014), whose concentrations can provide a

proxy for contributions from terrigenous materials (Webb and Kamber, 2000; Kamber *et al.*, 2004; Frimmel, 2009; Zhao *et al.*, 2009). A previous study has shown that Al and Th are the most insoluble (Taylor and McLennan, 1985). Thus, the changes of Al and Th concentrations in the marine carbonates are more sensitive to the influx of the terrigenous detritus. The Al and Th exhibits increased concentrations for the intervals with high terrigenous influx. Moreover, the ratios between elements with different solubilities can also trace the terrigenous influx. For the REE, the solubility increases from La to Lu. The REE patterns for the seawater and normal marine carbonate exhibit HREE enrichment, but that exhibit LREE enrichment for the terrigenous detritus (Kamber *et al.*, 2004; Frimmel, 2009; Zhao *et al.*, 2009). Thus, the HREE/LREE values of the marine carbonates can also indicate the influence of the terrigenous detritus. The HREE/LREE values exhibit decreased concentrations for the intervals with high terrigenous influx. As shown in Fig.5, HREE/LREE values in the reef carbonates are negatively associated with their Th and Al concentrations; however, it shows positive correlation between their Al and Th concentrations. This indicates that HREE/LREE values, Al concentrations, and Th concentrations of the reef carbonates are useful indexes for evaluating the influence on the seawater compositions from the terrigenous detritus in the study area.

Based on the geochemical characteristics of the trace element and REE compositions and $^{87}Sr/^{86}Sr$ values of the reef carbonates (the $^{87}Sr/^{86}Sr$ data are reported in another article, which is under review), 6 intervals can be divided (Fig.6); they are H1 (0–89.30 m, about 0–0.11 Myr), L1 (89.30–198.30 m, about 0.11–2.2 Myr), H2 (198.30–374.95 m, about 2.2–5.3 Myr), D (374.95–758.40 m, about 5.3–13.6 Myr), L2 (758.40–976.86 m, about 13.6–15.5 Myr), and H3 (976.86–1200.00 m, about 15.5–21.5 Myr). In the intervals of H1, H2, and H3, the HREE/LREE values are relatively low, whereas the Al, Th concentrations and the $^{87}Sr/^{86}Sr$ values are relatively high. In the intervals of L1 and L2, the HREE/LREE values are relatively high, whereas the Al, Th concentrations and $^{87}Sr/^{86}Sr$ values are relatively low. In the interval of D, the HREE/LREE values steadily increase with the depth, and the Al, Th concentrations and $^{87}Sr/^{86}Sr$ values decrease with the depth, although the amplitudes and rates of variation are relatively small. The lowest $^{87}Sr/^{86}Sr$ values in the reef carbonates generally coincide with the lowest values of Al, Th concentrations and highest values of HREE/LREE. This also indicates that HREE/LREE, Al concentrations, and Th concentrations are useful indexes for evaluating the influence on the seawater compositions from the terrigenous detritus in the study area. The relatively low HREE/LREE values and the relatively high Al, Th concentrations in the intervals of H1, H2, and H3 indicate the high terrigenous input into the SCS during these geological periods. On the contrary, the relatively high HREE/ LREE values and the relatively low Al, Th concentrations in the intervals of L1 and L2 indicate the contemporaneous terrigenous input into the SCS was relatively low.
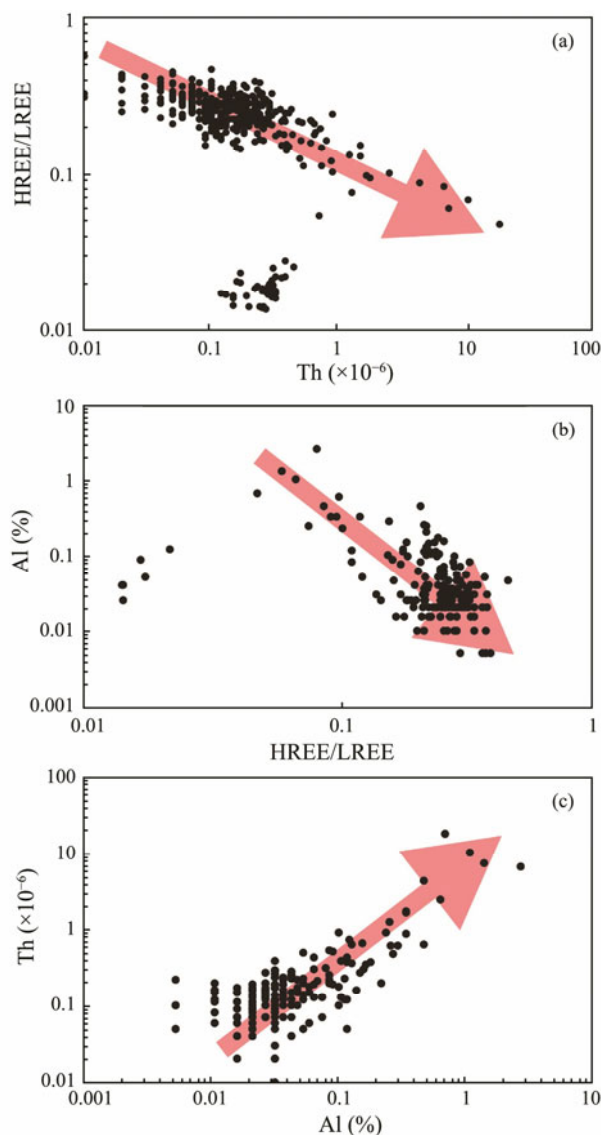
Fig.5 Cross plots of Th *vs*. HREE/LREE, Al *vs*. HREE/ LREE, and Al *vs*. Th for reef carbonates from the well 'Xike-1' reef core.

Because the trace element concentrations in terrigenous detritus are generally much higher than those of the pure carbonate, even a minor influence of the detritus can significantly elevate the trace element concentrations of carbonate (Zhao and Zheng, 2014). This may lead to a loss of the primary signature in pristine carbonates, which may be inevitable due to a change in the acid strength during the digestion of impure carbonates (Nothdurft *et al.*, 2004). As shown in Fig.7 and Table 2, the REE patterns of carbonate samples from the well 'Xike-1' reef core generally show seawater-like REE patters (left-leaning), but those degrees of left-leaning are lesser than that of seawater. The PAAS-normalized HREE/LREE values of the intervals H1, H2, and H3 (with an average of 2.01) are lesser than those of the intervals of L1 and L2 (with an average value of 2.98). This indicates that carbonate samples from the well 'Xike-1' reef core inherited the geochemical characteristics of paleoseawater, but they also influenced by the terrigenous detritus, especially for the carbonate samples in the intervals H1, H2, and H3.
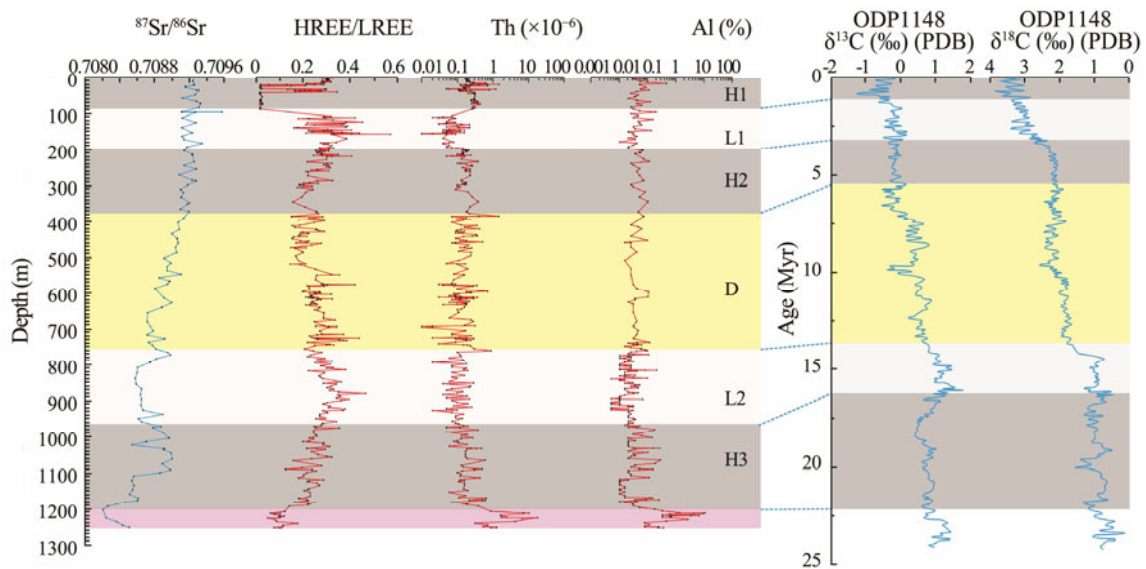
Fig.6 Changing curves of the HREE/LREE values, Al and Th concentrations, and ^{87}Sr/^{86}Sr values of reef carbonates from the well 'Xike-1' reef core. Changing curves of seawater δ^{13}C and δ^{18}O values in the SCS are also provided. The purple part was the segment below 1200 m. The HREE/LREE values are high in intervals H1, H2, and H3; and they are low in intervals L1 and L2; whereas they exhibit an upward in interval D. The δ^{13}C and δ^{18}O data in the benthonic foraminifera skeletons from the drill core of ODP site 1148 are derived from Zhao *et al.* (2001); Wang *et al.* (2003). The time and depth data of stratigraphic and chronologic boundaries are from Ma *et al.* (2015); Qiao *et al.* (2015); Wang *et al.* (2015); Xiu *et al.* (2015); You *et al.* (2015); Zhai *et al.* (2015); Zhao *et al.* (2015); Zhu *et al.* (2015); Bi *et al.* (2017).
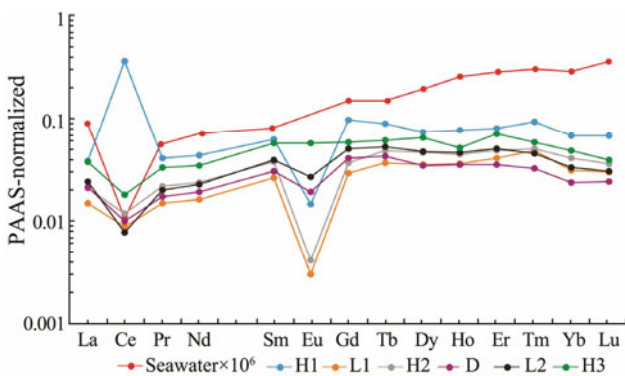

Fig.7 PAAS-normalized REE patterns for carbonates from 'Xike-1' reef core in the 6 intervals (L1, L2, D, H1, H2, and H3). Seawater REE data are from Kawabe *et al.* (1998), which has been enlarged 106 times.

5.3 Paleoenvironment

The depth data are transformed into chronologic data for further comparative analysis. The chronologic data of each points are calculated by weighted interpolation method, based on the chronologic data of the stratigraphic and chronologic boundaries which have been proven and affirmed (the changing curves of the seawater δ^{13}C and δ^{18}O values recorded by the benthonic foraminiferal skeletons from the drill core of ODP site 1148 in the SCS are also provided in Fig.6).

Carbon and oxygen isotopic compositions of foraminiferal skeletons have traditionally been the primary focus of the palaeoenvironmental studies, because these proxies allow the most direct insights into local palaeotempera-

tures and carbon cycle dynamics (Ullmann *et al.*, 2017). The oxygen isotopic compositions of seawater are the leading factors controlling the δ^{18}O values of the foraminiferal skeletons (Waelbroeck *et al.*, 2002; Li *et al.*, 2002). A larger amount of water with high ^{16}O/^{18}O values is frozen in the ice sheets, which results that the seawater δ^{18}O values are relatively high during the glacial period (Chappel and Shackleton, 1986). On the contrary, the seawater δ^{18}O values are relatively low during the warming period. Thus, seawater positive δ^{18}O excursions are usually hypothesized to have a genetic link to ancient glacial events on Earth. As shown in Fig.6, the changing trend of the HREE/LREE values in the reef carbonates has no obvious correspondence with that of seawater δ^{18}O values. This indicates that the influx of terrestrial detritus could be very high both in the warming period and glacial period. It has been known that wet and warm climates favor chemical weathering, whereas dry and cold climates favor physical weathering (Riebe *et al.*, 2004). Both the enhanced physical weathering due to the relative sea level declining in the glacial period and the enhanced chemical weathering in the warming period may lead to the increase of the terrigenous input into the SCS, and thus that the paleoclimatic changes are unlikely to be the dominant factor for the increase of terrigenous influx in the study area.

Many environmental and evolutionary events in Earth's history are accompanied by the global carbon cycle disturbance. Thus, carbon isotope stratigraphy is a valuable approach to elucidating the mechanisms of perturbation to ecologic environments (Huang *et al.*, 2012). However, the influencing factors of seawater δ^{13}C values are much

more complex than those of seawater $\delta^{18}O$ values (Li *et al.*, 2002). As shown in Fig.6, the lowest values of HREE/LREE values in the reef carbonates are associated with the lowest values of the seawater $\delta^{13}C$ values recorded by the benthonic foraminiferal skeletons from the drill core of ODP site 1148 in the SCS, and thus that the changes of the terrigenous influx should be an important factor affecting the changes of seawater $\delta^{13}C$ values in this area.

Factors controlling the terrigenous input at a single site include climate and tectonism (Kump and Arthur, 1997; Molnar, 2004). As mentioned above, the paleoclimatic changes are unlikely to be the dominant factor for the increase of terrigenous influx in the study area. Instead, rapid exhumation of high terrain (*e.g.*, the Qinghai-Tibet Plateau) should provide the justification for the increase in terrigenous influx. Therefore, the increase in terrigenous influx should be caused by the enhancement of erosion, weathering or transportation linked to the tectonic activities in this area.

5.4 Coupling Relationship Between the Changing Process of Terrigenous in Flux and the Uplifting Process of Qinghai-Tibet Plateau

The uplift of Qinghai-Tibet Plateau was a global geological event during the late Cenozoic, which was well recorded by the marine sedimentary system (Wang, 1995). The sediments of the Bengal Fan and the Indus River Fan, which were adjacent to the Qinghai-Tibet Plateau, were both derived from the continental weathering caused by the Qinghai-Tibet Plateau uplift (Johnson, 1994). The forming of the thick sediments in the Yinggehai Basin during the Quaternary was also thought to be the result of the eastward stretch of the Qinghai-Tibet plateau uplifting (Wang, 1995). The core data from DSDP (Deep Sea Drilling Project) indicated that the accumulation rate of the marine sediments suddenly increased at about 17 Myr, which also responds to the uplift event of Qinghai-Tibet Plateau (Davis *et al.*, 1977). These data indicate that the uplift of Qinghai-Tibet Plateau has important influence on the marine environments, and that the increase of riverine sediment influxes caused by the uplift of Qinghai-Tibet Plateau also has influence on the seawater compositions.

A previous research has shown that there is a coupling relationship among the subsidence (deposition) of Qiongdongnan Basin, the development of Xisha Islands and the uplift of Qinghai-Tibet Plateau, because these three events are highly consistent in the development time and process (Bi *et al.*, 2017). Moreover, both the subsidence (deposition) process of Qiongdongnan Basin and the development process of Xisha Islands can be divided into three phases corresponding to the three uplifting periods of Qinghai-Tibet Plateau, respectively. Among them, the period of about 16.0–23.0 Myr is the first uplifting phase of the Qinghai-Tibet Plateau, with relatively high uplifting rate; the period of about 5.5–16.0 Myr is the steady uplifting phase, with relatively low uplifting rate; and the period of about 0–5.5 Myr is the rapidly uplifting phase, with the highest uplifting rate.

The changing process of the HREE/LREE values and Al, Th concentrations in reef carbonates from the well 'Xike-1' reef core also can be divided into three phases, accordingly (Fig.6). Among them, the interval from H1 to H2 (about 0–5.3 Myr) is the fluctuating phase of the trace element and REE concentrations in the reef carbonates from 'Xike-1' reef core, and the Th, Al concentrations are high and the HREE/LREE values are low in this period; the interval from D to L2 (about 5.3–15.5 Myr) is the relatively stable phase, and the Al and Th concentrations are low and the HREE/LREE values are high in this period; the interval of H3 (about 15.5–21.5 Myr) is the rapidly changing phase, and the Th, Al concentrations are high and the HREE/LREE values are low in this period (Fig.8). As shown in Fig.8, the low HREE/LREE values in the reef carbonates are generally associated with the high uplifting rates of the Qinghai-Tibet Plateau; whereas the high values of those Th and Al concentrations are associated to the high uplifting rates of the Qinghai-Tibet Plateau.
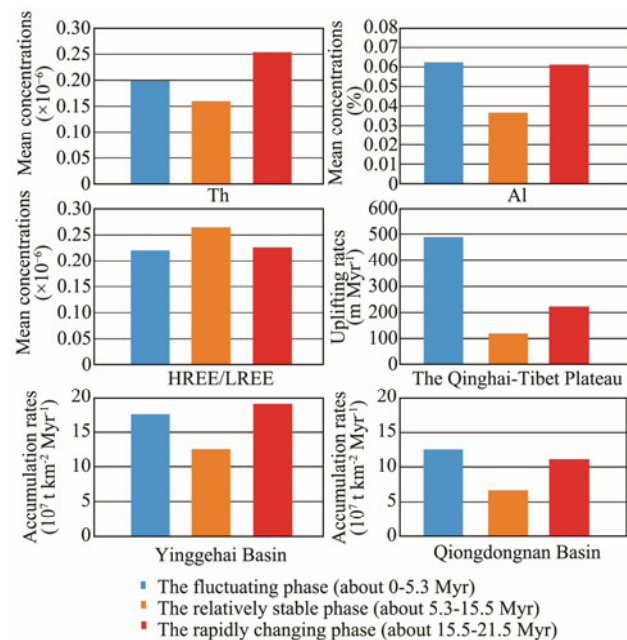

Fig.8 Average values of the Al, Th concentrations, HREE/LREE values and the uplifting rates of Qinghai-Tibet Plateau in three phases. The data of the Qinghai-Tibet Plateau uplifting rates are from Jiang and Li (2014). The data of the average accumulation rates of the sediments in the Yinggehai Basin and Qiongdongnan Basin are from Huang and Wang (2006).

Moreover, the high average accumulation rates of the sediments in the Yinggehai Basin and the Qiongdongnan Basin are generally associated with the high uplifting rates of the Qinghai-Tibet Plateau. This indicated a significant terrigenous contribution to the seawater composition of the SCS, which should be related to the changes of continental weathering area and terrigenous influx caused by the uplifting of Qinghai-Tibet Plateau. The uplift of Qinghai-Tibet Plateau has enlarged the continental weathering area, and thus more weathered continental materials were transported into the SCS by rivers and winds. There-

fore, the uplift of Qinghai-Tibet Plateau and the variations of uplifting rates should be the main factors controlling the variations of terrigenous influx.

6 Conclusions

1) The HREE/LREE values in the reef carbonates are negatively associated with their Th and Al concentrations; however, Al and Th concentrations show positive correlation. Moreover, the lowest $^{87}Sr/^{86}Sr$ values in the reef carbonates generally coincide with the lowest values of Al, Th concentrations and highest values of HREE/LREE. This feature indicates that the HREE/LREE values and Al, Th concentrations are good proxies for the influx of terrigenous materials in the SCS.

2) From top to bottom, the changing process of HREE/LREE values and Al, Th concentrations can be divided into 6 intervals; they are H1 (0–89.30 m, about 0–0.11 Myr), L1 (89.30–198.30 m, about 0.11–2.2 Myr), H2 (198.30–374.95 m, about 2.2–5.3 Myr), D (374.95–758.40 m, about 5.3–13.6 Myr), L2 (758.40–976.86 m, about 13.6–15.5 Myr), and H3 (976.86–1200.00 m, about 15.5–21.5 Myr).

3) The changing trend of the HREE/LREE values in the reef carbonates coincided with that of the seawater $\delta^{13}C$ values recorded by the benthonic foraminiferal skeletons from the drill core of ODP site 1148 in the SCS, but not with that of the seawater $\delta^{18}O$ values. This feature indicated that paleoclimatic changes are unlikely to be the dominant factor for the increase of terrigenous influx in the study area. Instead, the increase in terrigenous influx should be caused by the enhancement of erosion, weathering or transportation linked to the tectonic activities.

4) The low HREE/LREE values in the reef carbonates are generally associated with the high uplifting rates of the Qinghai-Tibet Plateau; whereas the high values of Th and Al concentrations are associated with the high uplifting rates of the Qinghai-Tibet Plateau. Therefore, the uplift of Qinghai-Tibet Plateau and the variations of uplifting rates should be the main factors controlling the variations of terrigenous influx.

Acknowledgements

References

Anagnostou, E., Sherrell, R. M., Gagnon, A., LaVigne, M., Field, M. P., and McDonough, W. F., 2011. Seawater nutrient and carbonate ion concentrations recorded as P/Ca, Ba/Ca, and U/Ca in the deep-sea coral *Desmophyllum dianthus*. *Geochimica et Cosmochimica Acta*, **75**: 2529-2543.

Armid, A., Asami, R., Fahmiati, T., Sheikh, M. A., Fujimura, H.,

Higuchi, T., Taira, E., Shinjo, R., and Oomori, T., 2011. Seawater temperature proxies based on D_{Sr}, D_{Mg}, and D_U from culture experiments using the branching coral Porites cylindrical. *Geochimica et Cosmochimica Acta*, **75**: 4273-4285.

Bachtel, S. L., Kissling, R. D., Martono, D., Rahardjanto, S. P., Dunn, P. A., and MacDonald, B. A., 2004. Seismic stratigraphic evolution of the Miocene-Pliocene Segitiga Platform, East Natuna Sea, Indonesia: The origin, growth, and demise of an isolated carbonate platform. In: *Seismic Imaging of Carbonate Reservoirs and Systems*. Erberli, G. P., *et al.*, eds., American Association of Petroleum Geologists, Tulsa, Oklahoma, 309-328.

Bi, D. J., Zhang, D. J., Zhai, S. K., Liu, X. Y., Xiu, C., Zhang, A. B., and Cao, J. Q., 2017. The coupling relationships among the Qinghai-Tibet Plateau uplifting, the Qiongdongnan Basin subsiding and the Xisha Islands' reefs developing. *Haiyang Xuebao*, **39** (1): 52-63 (in Chinese with English abstract).

Brand, U., and Veizer, J., 1980. Chemical diagenesis of a multicomponent carbonate system-1: Trace elements. *Journal of Sedimentary Research*, **50** (4): 1219-1236.

Brand, U., and Veizer, J., 1981. Chemical diagenesis of a multicomponent carbonate system-2: Stable isotopes. *Journal of Sedimentary Research*, **51** (3): 987-997.

Bruckschen, P., Bruhn, F., Meijer, J., Stephan, A., and Veizer, J., 1995. Diagenetic alteration of calcitic fossil shells: Proton microprobe (PIXE) as a trace element tool. *Nuclear Instruments and Methods in Physics Research Section B: Beam Interactions with Materials and Atoms*, **104** (1): 427-431.

Chappel, J., and Shackleton, N. J., 1986. Oxygen isotopes and sea level. *Nature*, **324** (6093): 134-140.

Chen, T., and Yu, K., 2011. P/Ca in coral skeleton as a geochemical proxy for seawater phosphorus variation in Daya Bay, northern South China Sea. *Marine Pollution Bulletin*, **62**: 2114-2121.

Davies, T. A., Hay, W. W., Southam, J. R., and Worsley, T. R., 1977. Estimates of Cenozoic oceanic sedimentation rates. *Science*, **197** (4298): 53-55.

Derry, L. A., Keto, L. S., Jacobsen, S. B., Knoll, A. H., and Swett, K., 1989. Sr isotopic variations in upper proterozoic carbonates from Svalbard and east Greenland. *Geochimica et Cosmochimica Acta*, **53** (9): 2331-2339.

Edwards, C. T., Saltzman, M. R., Leslie, S. A., Bergström, S. M., Sedlacek, A. R. C., Howard, A., Bauer, J. A., Sweet, W. C., and Young, S. A., 2015. Strontium isotope ($^{87}Sr/^{86}Sr$) stratigraphy of Ordovician bulk carbonate: Implications for preservation of primary seawater values. *Geological Society of America Bulletin*, **127** (9): B31149.1.

Frimmel, H. E., 2009. Trace element distribution in Neoproterozoic carbonates as palaeoenvironmental indicator. *Chemical Geology*, **258**: 338-353.

Hastings, D., Emerson, S., and Mix, A., 1996. Vanadium in foraminiferal calcite as a tracer for changes in the areal extent of reducing sediments. *Paleoceanography*, **11**: 665-678.

Hess, J., Bender, M. L., and Schilling, J. G., 1986. Evolution of the ratio of strontium-87 to strontium-86 in seawater from cretaceous to present. *Science*, **231** (4741): 979-984.

Huang, S. J., Huang, K. K., Jie, L., and Lan, Y. F., 2012. Carbon isotopic composition of early Triassic marine carbonates, eastern Sichuan Basin, China. *Science China: Earth Sciences*, **55** (12): 2026-2038.

Huang, S. J., Wang, C. M., Huang, P. P., Zou, M. L., Wang, Q. D., and Gao, X. Y., 2008. Scientific research frontiers and considerable questions of carbonate diagenesis. *Journal of Chengdu University of Technology (Science & Technology Edition)*,

35 (1): 1-10 (in Chinese with English abstract).

Huang, W., and Wang, P. X., 2006. The sedimentary quantity and distribution of the South China Sea since Oligocene. *Science China: Earth Sciences*, **36** (9): 822-829 (in Chinese with English abstract).

Jiang, X. D., and Li, Z. X., 2014. Seismic reflection data support episodic and simultaneous growth of the Tibetan Plateau since 25 Myr. *Nature Communications*, **5**: 5453-5459.

Johnson, M. R. W., 1994. Volume balance of erosional loss and sediment deposition related to Himalayan uplifts. *Journal of the Geological Society*, **151** (2): 217-220.

Kamber, B. S., Bolhar, R., and Webb, G. E., 2004. Geochemistry of late Archaean stromatolites from Zimbabwe: Evidence for microbial life in restricted epicontinental seas. *Precambrian Research*, **132**: 379-399.

Kaufman, A. J., and Knoll, A. H., 1995. Neoproterozoic variations in the C-isotopic composition of seawater: Stratigraphic and biogeochemical implications. *Precambrian Research*, **73** (1-4): 27-49.

Kaufman, A. J., Jacobsen, S. B., and Knoll, A. H., 1993. The Vendian record of Sr and C isotopic variations in seawater: Implications for tectonics and paleoclimate. *Earth and Planetary Science Letters*, **120** (3): 409-430.

Kaufman, A. J., Knoll, A. H., and Awramik, S. M., 1992. Biostratigraphic and chemostratigraphic correlation of Neoproterozoic sedimentary successions: Upper Tindir Group, northwestern Canada, as a test case. *Geology*, **20** (2): 181-185.

Kawabe, I., Toriumi, T., Ohta, A., and Miura, N., 1998. Monoisotopic REE abundances in seawater and the origin of seawater tetrad effect. *Geochemical Journal*, **32** (4): 213-229.

Korte, C., Kozur, H. W., Bruckschen, P., and Veizer, J., 2003. Strontium isotope evolution of late Permian and Triassic seawater. *Geochimica et Cosmochimica Acta*, **67** (1): 47-62.

Kump, L. R., and Arthur, M. A., 1997. Global chemical erosion during the Cenzooic: Weather ability balances the budgets. In: *Tectonic Uplift and Climate Change*. Ruddiman, W. F., ed., Plenum Press, New York, 399-426.

Li, D., Shields-Zhou, G. A., Ling, H. F., and Thirlwall, M., 2011. Dissolution methods for strontium isotope stratigraphy: Guidelines for the use of bulk carbonate and phosphorite rocks. *Chemical Geology*, **290** (3-4): 133-144.

Li, S. L., Li, S. Q., Yang, W. D., Chen, Y. X., and Long, J. P., 2002. Oxygen and carbon isotopic record of foraminiferal crusts from HY126EA1 hole in the continental shelf of the East China Sea. *Haiyang Xuebao*, **24** (3): 52-63 (in Chinese with English abstract).

Liu, J. N., Ye, Z. Z., Han, C. R., Liu, X. B., and Qu, G. S., 1997. Meteoric diagenesis in Pleistocene reef limestones of Xisha Islands, China. *Journal of Asian Earth Sciences*, **15** (6): 465-476.

Ma, Z. L., Zhu, Y. H., Liu, X. Y., Luo, W., Ma, R. F., and Xu, S. L., 2015. Quaternary calcareous alga and its ecological function from the ZK-1 well in Xisha Islands. *Earth Science – Journal of China University of Geoscience*, **40** (4): 718-724 (in Chinese with English abstract).

Molnar, P., 2004. Late Cenozoic increase in accumulation rates of terrestrial sediment: How might climate change have affected erosion rates? *Annual Review of Earth & Planetary Sciences*, **32**: 67-89.

Morford, J. L., and Emerson, S., 1999. The geochemistry of redox sensitive trace metals in sediments. *Geochimca et Cosmochimca Acta*, **63**: 1735-1750.

Nothdurft, L. D., Webb, G. E., and Kamber, B. S., 2004. Rare earth element geochemistry of late Devonian reefal carbonates, Canning Basin, western Australia: Confirmation of a seawater REE proxy in ancient limestones. *Geochimica et Cosmochimica Acta*, **68**: 263-283.

Qiao, P. J., Zhu, W. L., Shao, L., Zhang, D. J., Cheng, X. R., and Sun, Y. M., 2015. Carbonate stable isotope stratigraphy of well XK1, Xisha Islands. *Earth Science – Journal of China University of Geoscience*, **40** (4): 725-732 (in Chinese with English abstract).

Riebe, C. S., Kirchner, J. W., and Finkel, R. C., 2004. Erosional and climatic effects on long-term chemical weathering rates in granitic landscapes spanning diverse climate regimes. *Earth and Planetary Science Letters*, **224**: 547-562.

Sarnthein, M., Pflaumann, U., Wang, P. X., and Wong, H. K., 1994. Preliminary report on Sonne-95 cruise '*Monitor Monsoon*' to the South China Sea; Manila-Guangzhou-Hongkong-Kota Kinabalu-Hongkong; 16 April – 8 June 1994. Berichte-Reports. *Geologisch-Palaeontologisches Institut und Museum, Christian-Albrechts-Universitaet Kiel*, **68**: 5-39.

Shao, L., Cui, Y. C., Qiao, P. J., Zhang, D. J., Liu, X. Y., and Zhang, C. L., 2017. Sea-level changes and carbonate platform evolution of the Xisha Islands (South China Sea) since the early Miocene. *Palaeogeography, Palaeoclimatology, Palaeoecology*, **485** (1): 504-516.

Shi, X. B., Zhou, D., Qiu, X. L., and Zhang, Y. X., 2002. Thermal and rheological structures of the Xisha Trough, South China Sea. *Tectonophysics*, **351** (4): 285-300.

Taylor, S. R., and McLennan, S. M., 1985. *The Continental Crust: Its Composition and Evolution*. Blackwell, Oxford, 1-312.

Ullmann, C. V., Frei, R., Korte, C., and Lüter, C., 2017. Element/Ca, C and O isotope ratios in modern brachiopods: Species-specific signals of biomineralization. *Chemical Geology*, **460** (5): 15-24.

Umbgrove, J. H. F., 1947. Coral reefs of the East Indies. *Geological Society of America Bulletin*, **58** (8): 729-778.

Veizer, J., and Compston, W., 1976. $^{87}Sr/^{86}Sr$ in precambrian carbonates as an index of crustal evolution. *Geochimica et Cosmochimica Acta*, **40** (8): 905-914.

Waelbroeck, C., Labeyrie, L., Michel, E., Duplessy, J. C., Mcmanus, J. F., Lambeck, K., Balbona, E., and Labracheriee, M., 2002. Sea-level and deep water temperature changes derived from benthic foraminifera isotopic records. *Quaternary Science Reviews*, **21** (1): 295-305.

Wang, C. Y., He, X. X., and Qiu, S. Y., 1979. Preliminary study on the carbonate rocks and microfossils of the well 'Xiyong-1', Xisha Islands. *Petroleum Geology and Experiment*, **1**: 23-38 (in Chinese).

Wang, P. X., 1995. ODP and Qinghai-Tibet Plateau. *Advances in Earth Sciences*, **10** (3): 254-257 (in Chinese with English abstract).

Wang, P. X., Zhao, Q. H., Jian, Z. M., Cheng, R. X., Huang, W., Tian, J., Wang, J. L., Li, Q. Y., Li, B. H., and Su, X., 2003. The deep sea records of the past 30 Ma in the South China Sea. *Chinese Science Bulletin*, **48** (21): 2206-2215 (in Chinese with English abstract).

Wang, W., Guo, J., Cai, G., and Wang, D., 2018. Intelligent identification of remnant ridge edges in region west of Yongxing Island, South China Sea. *Journal of Ocean University of China*, **17** (1): 118-128.

Wang, Z. F., Cui, Y. C., Shao, L., Zhang, D. J., Dong, X. X., Liu, X. Y., Zhang, C. L., You, L., and Xiao, A. T., 2015. Carbonate platform development and sea level variations of Xisha Islands-based on BIT index results of Well XK1. *Earth Science – Journal of China University of Geoscience*, **40** (5): 900-908 (in Chinese with English abstract).

Webb, G. E., and Kamber, B. S., 2000. Rare earth elements in Holocene reefal microbialites: A new shallow seawater proxy. *Geochimca et Cosmochimca Acta*, **64**: 1557-1565.

Wei, G. J., Sun, M., Li, X., and Nie, B., 2000. Mg/Ca, Sr/Ca and U/Ca ratios of a porites coral from Sanya Bay, Hainan Island, South China Sea and their relationships to sea surface temperature. *Palaeogeography, Palaeoclimatology, Palaeoecology*, **162**: 59-74.

Xi, W., Fu, D. J., Yan, X. W., Zhu, Y. J., Zhao, G. C., Xi, L. Y., and Han, C. Y., 2005. Constraints on biogenetic reef formation during evolution of the South China Sea and exploration potential analysis. *Earth Science Frontiers*, **12** (3): 245-252.

Xia, K. Y., 1996. *The Geophysics and Oil & Gas Resources of the Nansha Islands and Their Adjacent Sea Area*. Science Press, Beijing, 113-120 (in Chinese).

Xie, Y., Wu, T., Sun, J., Zhang, H., Wang, J., Gao, J., and Chen, C., 2018. Sediment compaction and pore pressure prediction in deepwater basin of the South China Sea: Estimation from ODP and IODP drilling well data. *Journal of Ocean University of China*, **17** (1): 25-34.

Xiu, C., 2016. Reef development and environmental evolution in Shi Island, Xisha Islands since the Neogene. PhD thesis. Ocean University of China, 48-90.

Xiu, C., Luo, W., Yang, H. J., Zhai, S. K., Liu, X. Y., Cao, J. Q., Liu, X. F., Chen, H. Y., and Zhang, A. B., 2015. Carbonate stable isotope stratigraphy of well Xike-1, Xisha Islands. *Earth Science – Journal of China University of Geoscience*, **40** (4): 645-652 (in Chinese with English abstract).

You, L., Yu, Y. P., Liao, J., Liu, L., Liu, N., Zhao, S., and Li, X., 2015. Quaternary petrological characteristics and pore types and their formation mechanism near the typical exposed surface in Well Xike-1. *Earth Science – Journal of China University of Geoscience*, **40** (4): 671-676 (in Chinese with English abstract).

Zhai, S. K., Mi, L. J., Shen, X., Liu, X. Y., Xiu, C., Sun, Z. P., and Cao, J. Q., 2015. Mineral compositions and their environmental implications in reef of Shidao Island, Xisha. *Earth Science – Journal of China University of Geoscience*, **40** (4): 597-605 (in Chinese with English abstract).

Zhang, L., Li, W. C., and Zeng, X. H., 2003. Stratigraphic sequence and hydrocarbon potential in Lile Basin. *Petroleum Geology and Experiment*, **25** (5): 469-472 (in Chinese with English abstract).

Zhang, M. S., Liu, J., and Zhou, M. Q., 1994. Study on magnetic susceptibility of the well 'Xiyong-1'. *Chinese Science Bulletin*, **39** (4): 340-343 (in Chinese with English abstract).

Zhao, M. Y., and Zheng, Y. F., 2014. Marine carbonate records of terrigenous input into paleotethyan seawater: Geochemical constraints from carboniferous limestones. *Geochimica et Cosmochimica Acta*, **141**: 508-531.

Zhao, Q. H., and Wang, P. X., 1999. The advances on the Quaternary paleoceanography in the South China Sea. *Quaternary Sciences*, **6** (3): 481-501 (in Chinese with English abstract).

Zhao, Q. H., Jian, Z. M., Wang, J. L., Cheng, X. R., Huang, B. Q., Xu, J., Zhou, Z., Fang, D. Y., and Wang, P. X., 2001. Neogene oxygen isotopic stratigraphy, ODP Site 1148, northern South China Sea. *Science in China (Series D: Earth Sciences)*, **44** (10): 934-942.

Zhao, S., Zhang, D. J., Liu, L., You, L., Liu, N., Xiao, A. T., Yu, Y. P., and Li, X., 2015. Petrographic characteristics of Quaternary reef-carbonate diagnosis from Xike 1 well, the Xisha Islands, South China Sea. *Earth Science – Journal of China University of Geoscience*, **40** (5): 900-908 (in Chinese with English abstract).

Zhao, Y. Y., Zheng, Y. F., and Chen, F., 2009. Trace element and strontium isotope constraints on sedimentary environment of Ediacaran carbonates in southern Anhui, South China. *Chemical Geology*, **265**: 345-362.

Zhu, W. L., Wang, Z. F., Mi, L. J., Du, X. B., Xie, X. N., Lu, Y. C., Zhang, D. J., Sun, Z. P., Xiu, X. Y., and You, L., 2015. Sequence stratigraphic framework and reef growth unit of borehole XK-1 from Paracel Islands, South China Sea. *Earth Science – Journal of China University of Geoscience*, **40** (4): 677-687 (in Chinese with English abstract).

(Edited by Chen Wenwen)